Journal of Engineering Mathematics **35:** 135–147, 1999.

Radiation and diffraction analysis of the McIver toroid

J. N. NEWMAN
Department of Ocean Engineering, MIT, Cambridge (Mass.), U.S.A. e-mail: jnn@chf.mit.edu

Received 5 August 1997; accepted in revised form 7 April 1998

Abstract. A hydrodynamic analysis is performed of a special toroidal body which is known to have a nontrivial solution of the homogeneous linearized free-surface boundary-value problem with oscillatory time-dependence. This solution corresponds physically to unbounded resonant motion of the fluid in the 'moon pool' at the center of the toroid. The added mass, damping, and elevation of the free surface in the moon pool are computed for a range of wavenumbers, with singular results in the resonant regime.

Keywords: hydrodynamics, free surface, water waves, floating toroids, moon pools, trapped waves.

1. Introduction

In most cases of practical interest the linearized boundary-value problem for oscillatory motions of a floating body has a unique solution, for all frequencies and corresponding wavenumbers. John [1] proved uniqueness, subject to the geometric restriction that no vertical line intersects the submerged surface of the body more than once. Extensions of John's uniqueness proof have attracted frequent attention from mathematicians [2]. Counter-examples have been constructed for periodic solutions which extend to infinity in one horizontal direction, and for equivalent problems involving a compact body in a channel of finite width. Engineers have been less interested in this issue, on the presumption that relevant physical problems have a unique solution.

Recently it has been shown by McIver [2] that pairs of two-dimensional floating bodies can be constructed, with the remarkable property that solutions exist with homogeneous boundary conditions at a sequence of frequencies ω and corresponding wavenumbers k. The construction is very simple and uses a pair of point sources on the free surface separated by half a wavelength (more generally an integer plus a half times the wavelength). The radiated waves at infinity are canceled by interference, and the corresponding streamlines represent pairs of floating bodies enclosing the sources.

A similar procedure has been used by McIver and McIver [3] to derive a family of axisymmetric bodies from a three-dimensional ring source of radius $r = c$ in the free surface. There are no axisymmetric radiated waves if kc is a zero of the Bessel function $J_0(kr)$, and a family of stream surfaces can be constructed which enclose the ring source. We shall refer to these as 'McIver toroids.'

Since a nonzero solution exists near the body, and no radiated waves exist at infinity, these solutions are associated physically with 'trapped waves'. For brevity here we shall refer to them as 'homogeneous solutions', since the boundary conditions are homogeneous and no waves exist in the far field.

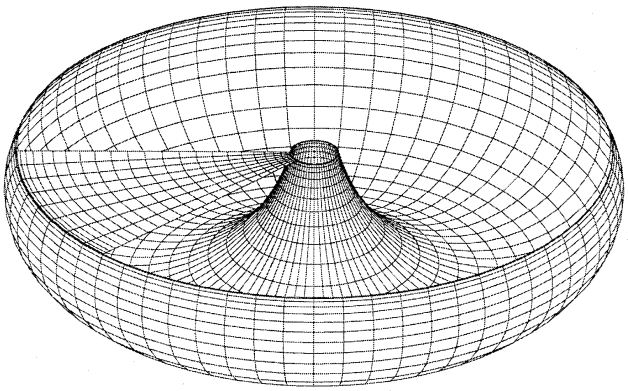

Figure 1. Perspective view of the McIver toroid. This view is from above the free surface, looking down inside the body. The free surface intersects the body at the outer and inner waterlines, which form the upper circular boundaries of the submerged surface. In addition to the submerged surface, a 45°-sector is shown of the interior free surface which is used for the removal of irregular-frequency effects. This toroid is generated from the outermost contour in Figure 2, with 32 cosine-spaced segments along the contour and 64 equally-spaced azimuthal segments, giving a total of 2048 panels on the submerged body surface.

Figure 1 shows a particular example of a McIver toroid, where a homogeneous solution exists at $kc = j_{0,1} = 2{\cdot}405\ldots$, the first zero of J_0. The free-surface elevation associated with this homogeneous solution is a slowly-varying function of the radius.

More generally, as noted by McIver and McIver [3], other families of body shapes can be constructed by setting the ring source radius to correspond to higher zeros of J_0. These will have associated homogeneous solutions at higher frequencies and wavenumbers analogous to the axisymmetric standing-wave modes in a closed basin. Similarly, Kuznetsov and McIver [4] consider the case where the ring source corresponds to a zero of J_m and the homogeneous solution is proportional to $\cos m\theta$, where θ denotes the azimuthal angle about the vertical z-axis.

Two geometric features of the McIver toroids are important in the context of a homogeneous solution. First, the maximum value of the outer radius occurs below the free surface, violating the restriction of John's uniqueness theorem. Secondly, there is an internal free surface which is totally enclosed by the surrounding body, and open to the exterior fluid domain beneath the body. We shall refer to this internal domain as a 'moon pool', following the jargon of offshore technology.

Vessels used for offshore operations are frequently constructed with moon pools, which generally are small relative to the horizontal dimensions of the body. Highly-tuned resonant oscillations can occur within moon pools, with important practical effects in terms of both local motions and global pressure forces. The first resonant mode (ordered in terms of increasing frequency ω and wavenumber k) is analogous to a Helmholtz resonance with predominantly vertical motion in the moon pool. It is usually referred to as the 'pumping mode' since the free surface moves in a similar manner to a piston. The higher-order modes correspond to standing waves within a vertical cylinder. If the moon pool is cylindrical, and its depth D is large compared to b, the pumping mode occurs when $kD \simeq 1$ [5, pp. 99–100]. This is the mode of primary importance in most practical cases.

The radiation damping of typical moon pools is small, but nonzero. Thus it is possible to compute the linear response characteristics, including the large-amplitude resonance, from

three-dimensional panel methods. In the resonant regime these results may be unrealistic, due to nonlinear and viscous effects, but the linear ideal-fluid analysis is still useful in predicting the frequencies at which resonance occurs, and the relative magnitude, in relation to the body geometry. Large numbers of panels must be used to obtain accurate results near the resonant wavenumbers. Newman [6] has presented results for a truncated circular cylinder of radius a and draft D, with a coaxial moon pool of radius $b < a$.

In this paper we describe numerical solutions of the radiation and diffraction problems for a McIver toroid. One motivation for this work is to provide independent evidence that nontrivial homogeneous solutions exist. In addition, we show how the existence of a homogeneous mode affects the response of these bodies, and the numerical evaluation of relevant hydrodynamic parameters. In the exact sense the solutions of both the radiation and diffraction problems are nonunique, but for small perturbations of the body shape, or wavenumber, these problems are well posed and a careful numerical analysis will yield results which can be interpreted in the limiting case to apply to the McIver toroids.

For simplicity and brevity we restrict our attention to the case of an axisymmetric ring source, and to the first zero of the Bessel function J_0. This is the case which corresponds to the pumping mode of a moon pool and is of the greatest practical interest. Higher-order modes and nonaxisymmetric modes also require greater computational efforts due to the larger values of the frequency and wavenumber. We expect that the resulting hydrodynamic response characteristics are qualitatively similar.

Since the homogeneous solution corresponds to an undamped free-surface elevation in the moon pool, any axisymmetric forcing at the same frequency is expected to give infinite response. This argument applies to both the heave radiation problem and to the diffraction of incident waves by the fixed body. Associated with this unbounded fluid motion one should expect a corresponding infinite pressure. Thus, the vertical exciting force due to incident waves is infinite, and similarly for the heave added-mass and damping coefficients. (At this stage we leave open the possibility that only one of the latter coefficients is unbounded, if the phase of the infinite pressure force coincides with either the velocity or acceleration of the heave motions. It will be shown subsequently that this possibility does not occur.)

This heuristic estimate of the heave damping is contrary to what one might conclude based on the fact that the homogeneous solution does not radiate waves in the far field. Thus, it might be argued that the heave damping at the resonant wavenumber is bounded. However, it is known from the Haskind relations that the heave damping coefficient of an axisymmetric body is directly proportional to the square of the exciting force, which is unbounded. Thus, we conclude that the heave damping coefficient of the McIver toroid is unbounded at resonance. The numerical results presented below support this conjecture.

The paper is organized as follows. First we rederive the geometry of the McIver toroids by a different numerical scheme. This complementary approach confirms the geometric results of McIver and McIver [3], and also facilitates generalizations including a ring source which is submerged, or in a fluid of finite depth. We use these results to construct discretized surfaces in terms of small quadrilateral flat panels, as illustrated in Figure 1, which are input to a panel program. Computations are performed to evaluate the added-mass, damping, and exciting-force coefficients, and the moon-pool elevation. These four hydrodynamic parameters all display singular behavior in the vicinity of the wavenumber where a homogeneous solution exists. The magnitude of the singular features increases as the geometric discretization is refined. This numerical evidence supports the fact that a homogeneous solution exists for the

exact body shape, and also permits us to study the hydrodynamic characteristics in the vicinity of resonance.

The computations here are performed by means of the low-order panel program WAMIT. A more effective procedure could be adopted, based on an axisymmetric code similar to those described by Hulme [7] and Fernandes [8], but this would require special development of an appropriate code.

2. Geometrical construction

The first task is to consider the velocity induced by a ring source of radius c. Except where otherwise noted the fluid depth is assumed infinite, and the ring source is in the plane of the free surface. The wavenumber k is fixed, with $kc = j_{0,1}$. Nondimensional coordinates are used hereafter, with $c = 1$. Thus, the ring source is a distribution of point sources around the unit circle.

In [3] the velocity potential for a ring source is evaluated from the special integral representation derived by Hulme [7]. The integration around the circle is carried out analytically, but the remaining semi-infinite integral in wavenumber space is evaluated numerically with a truncation correction. A complementary procedure is followed here, to take advantage of the subroutine for a point source based on the algorithms described in [9]. The contributions from the Rankine singularity $1/R$ and its image above the free surface are expressed by elliptic integrals. The remaining part of the free-surface point source is integrated around the ring using an adaptive Gauss–Chebyshev quadrature. The convergence tolerance of this scheme is 10^{-4}.

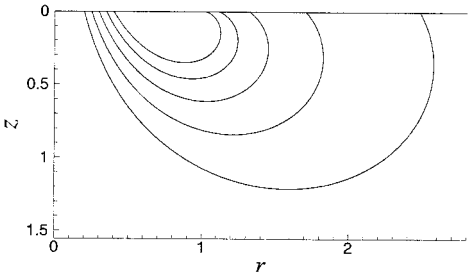

Figure 2. Contours of cross-sections generated by a ring source with unit radius in the free surface, in a fluid of infinite depth.

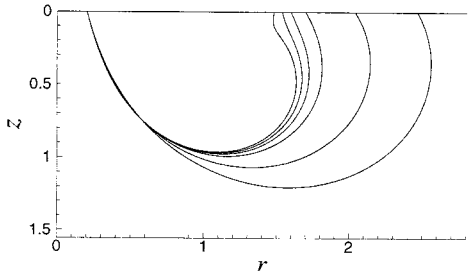

Figure 3. Contours of cross-sections generated by a ring submerged at the depth ζ below the free surface. Proceeding from the outermost to the innermost section the corresponding depths are $\zeta = 0$, 0·2, 0·25, 0·26, 0·265, 0·269. The fluid depth is infinite.

The oscillatory source strength is defined to be $q(t) = \mathrm{Re}(\mathrm{e}^{i\omega t})$, where Re denotes the real part, and the velocity potential is expressed as $\mathrm{Re}(\phi\, \mathrm{e}^{i\omega t})$. The potential factor ϕ is generally complex. However, when $J_0(kc) = 0$, there are no radiated waves in the far field, and the residue from the contour-integral representation of the potential is equal to zero. Thus, ϕ and its derivatives ϕ_r, ϕ_z are real. Here (r, θ, z) are circular cylindrical coordinates, with the z-axis positive downwards and $z = 0$ the plane of the free surface. The streamlines, defined by the relation $\phi_r\, \mathrm{d}z - \phi_z\, \mathrm{d}r = 0$, can be found by integration of either of the equivalent differential equations

$$\mathrm{d}r/\mathrm{d}z = \phi_r/\phi_z, \tag{1}$$

$$dz/dr = \phi_z/\phi_r. \tag{2}$$

The objective here is to solve (1) or (2) for the shape of the submerged body cross-section $r = R(z)$ between the inner and outer waterlines $R(0) = b$ and $R(0) = a$. Since the body must enclose the ring source at $r = 1$, it follows that $b < 1 < a$. The integration of (1–2) is started at a specified point $R(0) = b < 1$, and either (1) or (2) is selected so that the right-hand side is of magnitude $\leqslant 1$. Runge–Kutta integration is used with a prescribed finite differential increment Δ. If $|\phi_r| < |\phi_z|$ (1) is solved, with $|\delta z| = \Delta$, and conversely for (2) with $|\delta R| = \Delta$, Initially δz and δR are positive; their signs are reversed at the points of maximum draft and maximum radius, respectively. In the last step, where $R(0) = a$ is evaluated, Δ is reduced to avoid overshooting the free surface. The opposite procedure, starting at a and integrating to b, is used to find the limiting cases described below, where the streamlines are tangent to the plane $z = 0$ at $a = 1$.

The accuracy of this scheme is limited by the subroutine for the free-surface Green function, which has estimated errors for the spatial derivatives on the order of 10^{-4} or 10^{-5}. The geometrical convergence has been measured in terms of the computed value of the outer radius $R(0) = a$. For this radius the results from both 2nd and 4th-order Runge–Kutta algorithms differ by less than 0·0015 when $\Delta = 0{\cdot}01$, with practically no improvement for smaller values of Δ. Comparison has been made for the case $b = 0{\cdot}2$ with computations provided by P. McIver (private communication) based on the method described in [3]. The results agree within graphical accuracy at all points along the contour. Maximum differences on the order of 0·001 occur at the outer radius.

Figure 2 shows the family of computed cross-sections for values of b between 0·2 and 0·4. At a maximum limit $b \sim 0{\cdot}407$ the slope $dz/dr \to 0$ at the outer waterline. For larger values of b the streamlines do not enclose the source ring and hence cannot be interpreted as possible body surfaces. This is consistent with the limit $kb = 0{\cdot}98$ given by Kuznetsov and McIver [4].

Similar computations have been made for a ring source submerged at a depth ζ. The results for $b = 0{\cdot}2$ are shown in Figure 3. As the submergence increases there is little change in the contours initially, but as ζ approaches its limiting value the slope dr/dz changes sign near the outer waterline. For larger submergence the contour no longer encloses the source.

The same computational scheme can be used for a fluid of finite depth. Figure 4 shows the resulting contours for a ring source in the free surface with inner radius $b = 0{\cdot}2$, and fluid depth $h = (0{\cdot}36, 0{\cdot}5, 1{\cdot}0, 2{\cdot}0, \infty)$. As the depth is decreased the slope at the inner radius is practically unchanged, but the draft and outer radius are reduced substantially. The limiting maximum value of b is shown in Figure 5, as a function of the depth.

3. Radiation and diffraction analysis

In the radiation and diffraction problems the toroid is forced in oscillatory vertical heave motions, or fixed in the presence of plane incident waves, respectively. The corresponding boundary-value problems are well known, and briefly summarized as follows. The potential ϕ is a harmonic function of (r, θ, z) in the domain of the fluid. On the unperturbed free surface the linearized boundary condition $\omega^2\phi - g\phi_z = 0$ is satisfied, where g denotes the gravitational acceleration. The potential vanishes as $z \to \infty$ in a fluid of infinite depth, or satisfies the

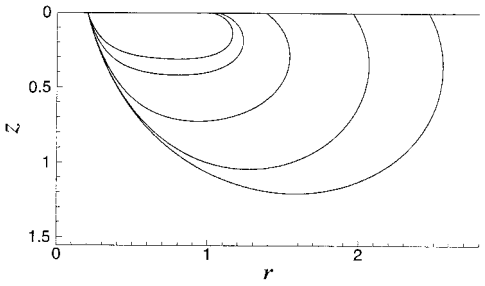

Figure 4. Contours of cross-sections generated by a ring source with unit radius in the free surface, in a fluid of depth h. Proceeding from the outermost to the innermost section the corresponding depths are $h = \infty$, 2·0, 1·0, 0·5, 0·36.

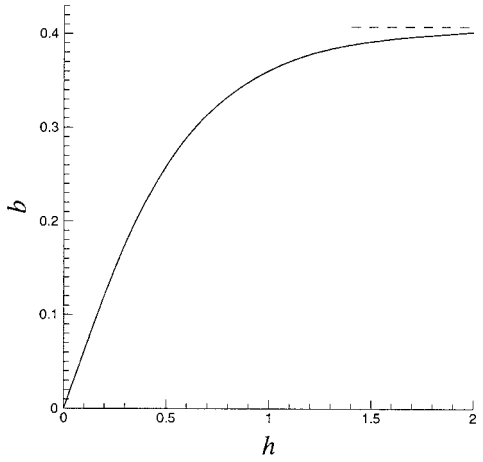

Figure 5. Limiting maximum value of the inner radius b as a function of the fluid depth h.

boundary condition $\phi_z = 0$ on the bottom $z = h$ in a fluid of finite depth. In the heave radiation problem the normal velocity $\phi_n = i\omega n_z$ on the body surface, where n_z is the vertical component of the unit normal vector, and the heave velocity is defined as $\mathrm{Re}(i\omega\, \mathrm{e}^{i\omega t})$. In the diffraction problem $\phi_n = 0$ on the body surface. The radiation condition $\phi_r \simeq -ik\phi$ is imposed as $r \to \infty$ for the radiation potential, and for the scattered component $\phi - \phi_I$ in the diffraction problem, where ϕ_I is the potential of the incident plane wave.

Following the boundary-integral-equation method, we derive the potential on the body surface as the solution of an integral equation which follows from Green's theorem. The potential of a point source beneath the free surface is used as the Green function, reducing the domain of the integral equation to the body surface. However, this reduction leads to the existence of a discrete set of irregular frequencies where the solution of the integral equation is nonunique. The irregular frequencies require special attention since they may be interspersed with the physically relevant resonances of the McIver toroid.

Homogeneous solutions of the integral equation exist at the irregular frequencies, although the solution of the full boundary-value problem is generally unique under these circumstances. The nonuniqueness of the integral equation is associated with the complementary boundary-value problem in the *interior* of the body with the same free-surface boundary condition on $z = 0$ and a homogeneous Dirichlet condition $\phi = 0$ on the inside surface of the body below $z = 0$. (This is the nonphysical domain inside the body, not to be confused with the fluid in the moon pool which is a part of the external domain outside the body surface.) The irregular frequencies have no physical significance, and it is necessary to remove their influence from the numerical solution. This can be achieved by extending the domain of the integral equation to include the plane $z = 0$ inside the body, where the additional boundary condition $\phi_z = 0$ is imposed, as described by Lee *et al.* [10].

We may estimate the values of the irregular frequencies by considering the simpler case of a truncated circular cylinder with outer radius a, moon-pool radius b, and draft D. It follows

Table 1. Number of panels on the body, interior free surface, and total, for the three discretizations used.

Body panels	512	2048	8192
Free-surface panels	384	1600	6656
Total panels	896	3648	14848

from separation of variables that the complementary potential can be expanded in terms of the eigenfunctions

$$\begin{pmatrix} J_m(\kappa r) \\ Y_m(\kappa r) \end{pmatrix} \begin{pmatrix} \cos\, m\theta \\ \sin\, m\theta \end{pmatrix} \sinh\, \kappa(z - D).$$

Since this potential must vanish on $r = a$ and $r = b$, the wavenumber κ is a root of the equation

$$J_m(\kappa a)Y_m(\kappa b) - Y_m(\kappa a)J_m(\kappa b) = 0. \tag{3}$$

The corresponding frequencies are determined from the interior free-surface condition in the form

$$\omega^2 = g\kappa\, \coth\, \kappa D. \tag{4}$$

To approximate the particular toroid used below we set $b = 0{\cdot}2$, $a = 2{\cdot}5$, and $D = 1{\cdot}0$. In this case the first two roots of (3) for $m = 0$ are $\kappa a = 3{\cdot}22$ and $6{\cdot}69$. In the case of infinite fluid depth the corresponding values of the exterior wavenumber $k = \omega^2/g$ are $k = 1{\cdot}51$ and $2{\cdot}81$.

The panel code WAMIT is used to compute numerical solutions of the integral equation. For this purpose the body surface is replaced by a finite number N of flat panels, and the potential is assumed to be constant on each panel. The integral equation is solved by collocation at the panel centroids, leading to a linear system of N algebraic equations for the potential on each panel. The code includes an option to solve the extended integral equation including the interior free surface, to permit removal of the irregular-frequency effects. Except where otherwise stated, this option has been used for the results presented here.

The results presented below are for the toroid shown in Figure 1. Three discretizations are used with 512, 2048, and 8192 panels on the submerged body surface. In the computations where irregular-frequency effects are removed the free surface inside the body is discretized with the same azimuthal subdivision. The radial subdivision is nonuniform with the width of the panels adjacent to the inner and outer waterlines equal to the width of the contiguous panels below the outer waterline, and with cosine spacing used to increase the width of the intermediate panels in a continuous manner. The total number of panels including both the physical submerged body surface and the interior free surface is shown in Table 1, for each of the three discretizations. In the computations two planes of geometric symmetry are imposed, corresponding to $\theta = (0, \pi)$ and $\theta = \pm\pi/2$. Only the component of ϕ which is symmetric about both planes is computed, since this is sufficient to evaluate the vertical force coefficients

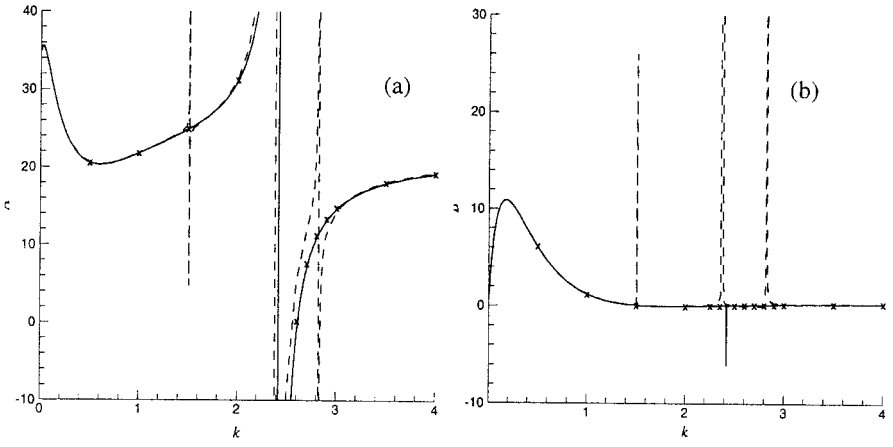

Figure 6. Heave added-mass (a) and damping (b) coefficients. The dashed curves include irregular-frequency effects, which are removed in the solid curves. Both curves are based on computations using the discretization shown in Figure 1 with 2048 panels on the body. The × marks represent computations with a total of 8192 panels on the body, and with the irregular-frequency effects removed.

and the free-surface elevation at $r = 0$. Thus the number of unknowns is one-quarter of the total number of panels.

The principal hydrodynamic parameters evaluated include the heave added-mass and damping coefficients, exciting-force, and the free-surface elevation at the center of the moon pool in the diffraction problem. The added-mass and damping coefficients are nondimensionalized by the factors ρc^3 and $\rho c^3 \omega$, respectively, where ρ is the fluid density and c the radius of the ring source. The exciting force is nondimensionalized by the factor $\rho g c^2 A$, where A is the incident-wave amplitude. The free-surface elevation is nondimensionalized by A.

Figures 6–7 show the values of the added mass, damping, and moon-pool elevation for wavenumbers in the range $(0 < kc < 4)$. Between 100 and 200 closely-spaced wavenumbers have been used for these computations, to define the details shown. Two sets of curves are included, where the effects of irregular frequencies are present (dashed) and where these effects are removed (solid), to emphasize the distinction between the irregular frequencies and the physically relevant moon-pool resonance. The resonance, which occurs near the theoretical value $k = j_{0,1}$, is present in both sets of curves. The two extra singularities in the dashed curves are due to the irregular-frequency effects, and coincide with the estimates $k = 1{\cdot}51$ and $2{\cdot}81$ based on (4).

Figure 8 shows the exciting force in the same wavenumber range, evaluated both directly from integration of the diffraction pressure, and indirectly using the Haskind relations. Differences between the two methods are noticeable in the vicinity of the resonant wavenumber, where the diffraction exciting force has a very sharp peak. The bandwidth of the Haskind peak is larger. The exciting force and damping vanish at $k = 1{\cdot}84\ldots$; a similar zero was noted in [6] for cylindrical bodies with moon pools.

The precise wavenumber where resonance occurs depends on the number of panels, and differs according as whether or not the irregular-frequency removal algorithm is, or is not, used. Figure 9 shows the wavenumber at which resonance occurs in each case, determined from the values of k at which the added mass passes through zero and the other parameters achieve their maximum amplitudes. As the number of panels increases, both resonant

wavenumbers tend to the correct theoretical value, with errors which appear to be inversely proportional to the number of panels.

The curves in Figures 6–8 are based on computations using the discretization with 2048 panels on the body. Also shown are discrete points for the more accurate representation using 8192 panels on the body. Comparison of these results indicates that the 2048-panel discretization gives results within graphical precision, except for small differences in the vicinity of the resonant wavenumber. Comparison (not shown) with the results using 512 panels indicates that these are less accurate, as expected. In general it appears that the computations converge to the exact theoretical solution, except in the vicinity of the resonant wavenumber where a more detailed comparison is required.

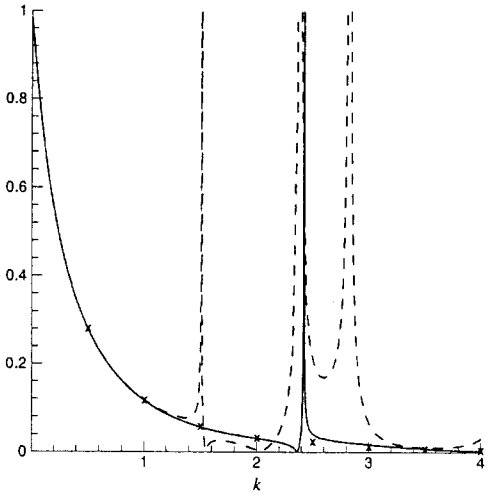

Figure 7. Amplitude of the free-surface elevation at the moon-pool center for the body fixed in incident waves. The dashed curves include irregular-frequency effects, which are removed in the solid curves. Both curves are based on computations using the discretization shown in Figure 1 with 2048 panels on the body. The × marks represent computations with a total of 8192 panels on the body, and with the irregular-frequency effects removed.

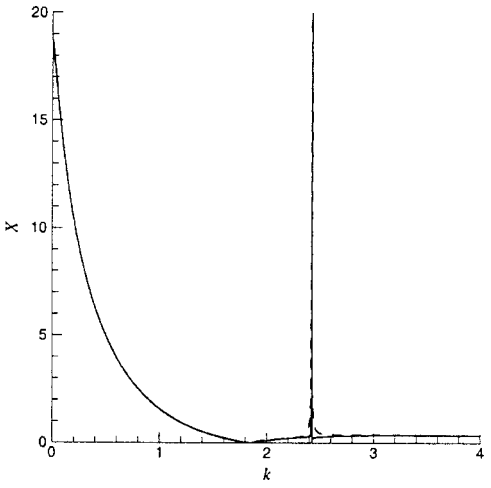

Figure 8. Heave exciting force coefficient based on direct integration of the diffraction pressure (solid curve) and on the Haskind relations (dashed curve). Both curves are based on computations using the discretization shown in Figure 1 with 2048 panels on the body, and with the irregular-frequency effects removed.

A theoretical explanation of the results in the vicinity of the resonant wavenumber can be developed, along similar lines to the explanations of large finite added-mass and damping variations [11, 12] for bodies in channels, or submerged beneath the free surface. Thus, we assume that the solution matrix is singular, with a simple pole in the complex wavenumber plane where the determinant of the discretized linear system is equal to zero. With the complex time factor $e^{i\omega t}$ the pole is generally above the real axis, but for the exact McIver toroid the pole is on the real axis, at $k = k_0 = j_{0,1}$. Each discretized body corresponds to a perturbation of the toroid with the pole shifted above the real axis by a small distance ϵ. As the number of panels tends to infinity, $\epsilon \to 0$. These assumptions imply that the velocity potential is of the form

$$\phi = \bar{\phi}(k) + \frac{\phi_0}{k - (k_0 + i\epsilon)}, \tag{5}$$

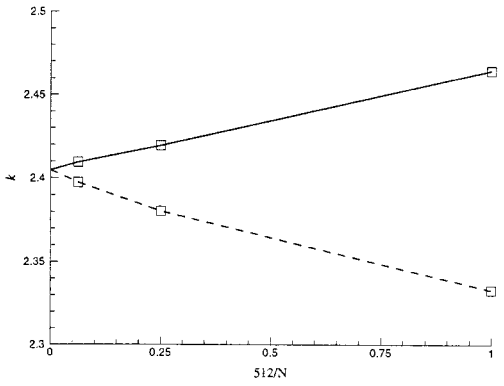

Figure 9. Values of the resonant wavenumber for each discretization, showing the convergence to the theoretical limit $j_{0,1} = 2{\cdot}4048\ldots$. The dashed curve is based on computations including the irregular-frequency effects, which are removed in the results shown by the solid curve.

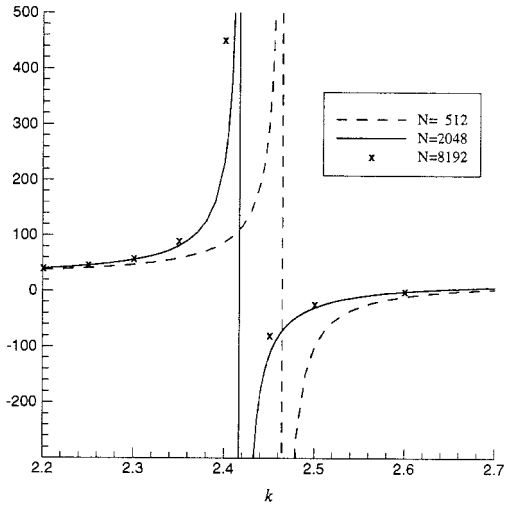

Figure 10. Added mass in the vicinity of resonance, showing the convergence of results using 512 (dashed curve), 2048 (solid curve), and 8192 ($\times$) panels on the body surface. The irregular-frequency effects are removed in all cases.

where $\bar{\phi}(k)$ is bounded and ϕ_0 does not depend on k. The integrated pressure force will have a corresponding form.

For the heave radiation problem the nondimensional added-mass and damping coefficients are the real and imaginary parts of the complex quantity $A + iB$. Since the complex force coefficient $A - iB$ is analytic in the lower half-plane, and $B > 0$, it follows that

$$A = \bar{A} + A_0 \frac{k - k_0}{(k - k_0)^2 + \epsilon^2}, \tag{6}$$

$$B = \bar{B} + B_0 \frac{\epsilon}{(k - k_0)^2 + \epsilon^2}, \tag{7}$$

where $\bar{A}$ and $\bar{B}$ are bounded, $B_0 > 0$, and $A_0 = -B_0$. For $\epsilon \ll 1$ these formulae are consistent with the results shown in Figure 6. Thus, for increasing values of the wavenumber, the added mass tends to a large positive value before changing sign abruptly, near $k = 2{\cdot}4$, and subsequently returns from a large negative value to normal positive values in accordance with the estimate (6). This rapid variation occurs over a relatively broad range of wavenumbers, determined by the magnitude of A_0 and independent of ϵ. On the other hand, the damping coefficient has a sharp 'spike' with bandwidth proportional to ϵ and peak value B_0/ϵ, equivalent to a finite delta function and consistent with (7).

The exciting force X can be evaluated either directly, from integration of the diffraction pressure, or from the radiation solution using the Haskind relations. For an axisymmetric body the Haskind relations can be used to show that the damping coefficient is proportional to $|X|^2$, and thus from (7)

$$X = \bar{X} + X_0 \left(\frac{\epsilon}{(k - k_0)^2 + \epsilon^2} \right)^{1/2}. \tag{8}$$

It follows that the singularity in the exciting force is weaker than for the damping coefficient, but with the same property that the bandwidth is $O(\epsilon)$. Since the diffraction pressure is singular in the same manner, the amplitude of the free-surface elevation in the moon pool is similar to (8). This conclusion is consistent with the results shown in Figure 7, but not with the assumed form of the potential (5), which has a stronger singularity. This contradiction suggests that the singularity of the inverse matrix is orthogonal to the normal velocity induced by the incident wave system at the resonant wavenumber. (Alternatively, one might consider the possibility that the singularity of the potential is orthogonal to the normal component n_z on the body surface, but that would imply a different form of the singular potential in the radiation and diffraction problems, contradictory to the assumption that in both cases the singular solution corresponds to the homogeneous solution of McIver and McIver [3].)

Figure 10 shows the added mass in the vicinity of resonance, and compares the results based on the three different discretizations. For $k \neq k_0$ the results show convergence as the number of panels increases, but as $k \to k_0$ the number of panels must be increased to achieve a given accuracy. With respect to the convergence of the damping and moon-pool resonance, the magnitude of the computed peak values increase and the bandwidth decreases, with increasing numbers of panels. However, the quantitative values are not considered to be reliable due to the proximity to resonance. Examples of inaccurate results are the negative damping peak shown in Figure 6(b), and the lack of agreement (not shown) between the peak values of the exciting force computed from the diffraction pressure and from the Haskind relations.

4. Computational notes

The nonvertical profile of the McIver toroid at the free surface is a feature which requires special attention in the computations. The use of a nonuniform discretization with relatively small panels at the waterline, as shown in Figure 1, helps to alleviate this problem. In addition, the logarithmic singularity in the free-surface Green function has been integrated analytically over each panel, following the procedure outlined in [13]. In preliminary computations, performed without removal of the logarithmic singularity, negative damping coefficients were more prevalent in the vicinity of resonance.

The iterative solver normally used for the solution of the linear system did not give consistent convergence in the vicinity of the resonant wavenumber and irregular frequencies. For that reason, direct Gauss elimination was used for all computations.

The computations reported here were performed on a Pentium 200 MHz PC and on a DEC Alpha 600 (5/33) workstation. Computing times ranged from a few seconds to a few hours per wavenumber, depending on the number of panels and irregular-frequency option.

5. Discussion of results

The computational results presented here support and extend the analysis of McIver and McIver [3]. The toroidal bodies illustrated in Figures 1 and 2, which coincide with the streamlines generated by a ring source, have singular hydrodynamic characteristics near the wavenumber $k = j_{0,1}$ where the ring source is wave-free. Since a homogeneous solution exists at this wavenumber, the exact solutions of the radiation and diffraction problems are not unique. The computations with increasing numbers of panels give a sequence of results which are progressively more singular. The hydrodynamic parameters converge, with increasing numbers of

panels, provided the wavenumber differs from k_0 by a fixed amount. As $k \to j_{0,1}$ the number of panels must be increased to achieve a specified accuracy. The values of $k = k_0$ where the computed results are singular converge to the theoretical value $j_{0,1}$.

The damping, exciting force, and elevation in the moon-pool all exhibit sharp peaks with narrow bandwidth at the resonant wavenumber. The spectral area associated with the damping peak appears to tend to a finite limit as the number of panels increases, suggesting that this singularity is equivalent to a delta function. The exciting force and moon-pool elevation have weaker singularities, and their spectral areas decrease with increasing numbers of panels. These conclusions are somewhat speculative, since the numerical solution is inaccurate within the narrow range of wavenumbers where these parameters are singular.

The singularity of the added mass is fundamentally different. As indicated in (6) this parameter has a simple pole, with variation between large positive and negative values occurring over a relatively broad bandwidth which does not decrease as the number of panels increases. This is confirmed by the comparisons shown in Figure 10, and there is no uncertainty in the quantitative values of these curves. Thus one can determine the 'residue' coefficient $A_0 \simeq -4$ in (6) with some confidence. This implies a spectral area of the damping-coefficient delta function equal to 4π, remarkably close to integrated values from the computed values of the damping coefficient *without removal of the irregular frequency effects*. With the irregular frequencies removed, the peak values of the damping are negative, and thus cannot be used reliably. No explanation has been found for this inconsistency, but it does serve as an example of the singular nature of the McIver toroid, and the effect of the homogeneous solution which exists at the critical wavenumber.

The results shown in Section 3 are for the toroid with inner radius $b = 0{\cdot}2$ and outer radius $a = 2{\cdot}49$. For larger values of b the outer radius decreases, and conversely, as indicated in Figure 2. The resonant wavenumber is unchanged, but the irregular frequencies increase when a decreases, and vice versa. When $b \simeq 0{\cdot}25$ the first irregular frequency is practically coincident with the resonant wavenumber. Limited computations have been performed in this regime, with and without removal of the irregular-frequency effects. In the latter case the moon-pool elevation contains two adjacent peaks which are relatively broad, where one corresponds to the irregular frequency and the other to the resonant wavenumber. These appear to remain distinct from each other as b is varied by small amounts, rather than coalescing into a single peak. With the irregular-frequency effects removed a single resonant peak is recovered, similar to the solid curve in Figure 7 but with a narrower bandwidth.

All of the results presented here are for the case of infinite fluid depth h. Qualitatively similar results have been computed for $h = 1$, using the corresponding profile shown in Figure 4. No computations have been performed for the submerged ring source, where the geometry is specified by the curves in Figure 3, but no fundamental difficulties are anticipated and similar results are expected. Similar results are also expected for the higher-order resonant wavenumbers $k = j_{0,m}$ corresponding to axisymmetric standing waves in the moon pool, and for higher-harmonic modes, corresponding to the more general body shapes described in [3] and [4].

References

1. F. John, On the motion of floating bodies, I, II. *Comm. Pure Appl. Math.* 2 (1949) 13–57, 3 (1950) 45–101.
2. M. McIver, An example of non-uniqueness in the two-dimensional linear water wave problem. *J. Fluid Mech.* 315 (1996) 257–266.

3. P. McIver and M. McIver, Trapped modes in an axisymmetric water-wave problem. *Quart. J. Mech. Appl. Math.* (to appear).
4. N. Kuznetsov and M. McIver, On uniqueness and trapped modes in the water-wave problem for a surface-piercing axisymmetric body. *Quart. J. Mech. Appl. Math.* (to appear).
5. O. M. Faltinsen, *Sea Loads on Ships and Offshore Structures.* Cambridge, UK: Cambridge University Press (1990) 328pp.
6. J. N. Newman, Recent results from numerical model tests. Int. Conf. 'Nonlinear Design Aspects of Physical Model Tests', Offshore Technology Research Center, Texas A & M University, College Station, Texas, U.S.A. (1997).
7. A. Hulme, A ring-source/integral-equation method for the calculation of hydrodynamic forces exerted on floating bodies of revolution. *J. Fluid Mech.* 128 (1983) 387–412.
8. A. C. Fernandes, *Analysis of an Axisymmetric Pneumatic Buoy by Reciprocity Relations and a Ring-Source Method.* Ph.D. Thesis, MIT, Cambridge, Mass. (1983) 183pp.
9. J. N. Newman, Approximation of free-surface Green functions. In: P. A. Martin and G. R. Wickham (eds), *Wave Asymptotics.* Cambridge, UK: Cambridge University Press (1992) pp. 107–135.
10. C.-H. Lee, J. N. Newman, and X. Zhu, An extended boundary integral equation method for the removal of irregular frequency effects. *Int. J. Num. Methods in Fluids* 23 (1996) 637–660.
11. C. M. Linton and D. V. Evans, Hydrodynamic characteristics of bodies in channels. *J. Fluid Mech.* 252 (1993) 647–666.
12. P. A. Martin and L. Farina, Radiation of water waves by a heaving submerged horizontal disc. *J. Fluid Mech.* 337 (1997) 365–379.
13. J. N. Newman and P. D. Sclavounos, The computation of wave loads on large offshore structures. In: T. Moan, N. Janbu and O. Faltinsen (eds), *Conference on the Behaviour of Offshore Structures (BOSS '88)*. Trondheim: Tapir Publishers. Vol. 2 (1988) pp. 605–622.